A Periodic Density Functional Theory Study of Intermolecular Isomerization of Toluene and Benzene Catalyzed by Acidic Mordenite Zeolite: Effect of the Zeolite Steric Constraints

Xavier Rozanska,*,† Rutger A. van Santen,† and François Hutschka§

Schuit Institute of Catalysis, Laboratory of Inorganic Chemistry and Catalysis, Eindhoven University of Technology, P.O. Box 513, 5600 MB Eindhoven, The Netherlands, and TotalFinaElf, Centre Européen de Recherche et Technique, Département Chimie des Procédés, B.P. 27, 76700 Harfleur, France

Received: November 9, 2001; In Final Form: March 5, 2002

A periodic density functional theory study of the isomerization reactions of toluene and benzene catalyzed by acidic mordenite is reported. Reaction energy diagrams including transition-state energies of disproportionation and direct transalkylation reactions are presented and analyzed. Alternative reaction pathways have been considered. The use of periodic structure calculations allows analysis of steric constraints that occur within zeolite micropores. General rules concerning the influence of steric constraints in relation with reaction mechanism are described.

1. Introduction

Transalkylation and isomerization of aromatics are important to petrochemistry and chemistry.[1] Appropriate catalysts for use in these processes are acidic zeolites. Zeolites are microporous aluminosilicates.[2] They were first employed to catalyze hydrotreating of petroleum feedstock on an industrial scale during the 1960s.[3] We will not extensively describe all of the properties that are bases to use zeolites as catalysts because these have already been extensively described elsewhere.[1−4] We will however focus on a few of them. One of the most important characteristics of zeolites as catalysts is their very high selectivity for many hydrocarbon reactions.[1a,1b,5] This is particularly true for the production of alkylated aromatics. For instance, in the case of xylene isomers, a high selectivity for *para*-xylene is desirable because this compound is used as a reactant in the textile synthesis industry.[1b] Zeolite catalysts can successfully be employed to realize this objective.[1]

The source of zeolite selectivity has been investigated since its first use.[5] It originates mainly from shape selectivity. The microporous network of zeolite is well-defined and different from one zeolite to another. This is the reason for higher diffusion rates of specific molecules compared to other molecules of different shape and size.[6] Zeolites were used as molecular sieves before they were considered as catalysts.[2b] Zeolite selectivity may also result from a difference in substrate reactivity. Depending on the micropore dimension as well as the location of the catalytic sites, some reaction pathways can be hampered with respect to others.[5,7] The nature of the catalytic site has also some influence on selectivity,[8] but we will not consider this situation in the present study. We will restrict our calculations to a single class of zeolitic catalytic sites, namely, the Brønsted acidic sites that are generated when framework Si^{IV} is substituted by Al^{III}.

In this study, we will investigate the intermolecular isomerization, or bimolecular transalkylation, between toluene and benzene.[9] This system will be used as a model of the intermolecular isomerization reaction between toluene molecules. The isomerization of aromatics has extensively been experimentally studied. It constitutes an ideal reaction to analyze the basis for the selectivity difference found for acidic zeolite catalysts. Aromatic isomerization may proceed via two alternative reaction pathways. According to Young et al.,[9c] the reaction can occur via an alkyl shift reaction or via a disproportionation reaction with diphenylmethane as intermediate. For MOR or ZSM-5, Guisnet et al.[9b,9d] and Corma et al.[10] have shown that isomerization via the shift mechanism is preferred rather than reaction via a disproportionation mechanism. The situation is different in the cases of faujasite, or zeolite Y, within which reaction appears to occur via the diphenylmethane intermediate.[9b,9d,10]

We recently conducted a theoretical study of these different reaction pathways by means of the cluster approach method.[11] The cluster approach method, within its well-known limitations (namely, an overestimation of the activation energies and an impossibility of analyzing transition-state selectivity because of the nondescription of the zeolite framework[12]), is a convenient approach with which to obtain qualitative data.[11,13−14] These results supported the experimentally observed reaction mechanism mentioned above. The disproportionation reaction pathway is part of a catalytic cycle, contrary to the shift isomerization reaction, which can be better described as a single reaction step. It is energetically costly to initiate the disproportionation catalytic cycle, but its continuation is easier than a shift isomer. However, this conclusion is only valid when the reaction is not controlled by transition-state selectivity. The cluster approach model does not include micropore-related information. Experimentally, the prediction based on these results should correspond to the chemistry of large pore zeolite catalysts.[9−10]

For comparison, we also report a periodic structure theoretical study of intramolecular isomerization of toluene and xylene isomers catalyzed by acidic mordenite.[14] It is interesting to compare these data with intermolecular isomerization of aromatics catalyzed by acidic mordenite because of strong experimental evidence that transition-state selectivity totally[15] or partly[9,10] prohibits this reaction pathway. In this study, we will also

* To whom correspondence should be addressed. Fax: +31 40 245 5054. E-mail: tgakxr@chem.tue.nl.
† Schuit Institute of Catalysis.
§ Centre Européen de Recherche et Technique.

10.1021/jp014125h CCC: $22.00
Published on Web 03/30/2002

analyze how transition-state selectivity affects the bimolecular isomerization reaction selectivity. We will use the same method and zeolitic model as in the previous study.[7,14] This will considerably simplify comparison between the calculated data of the previous and the present study.

2. Methods

The Vienna ab initio simulation package (VASP) was used to perform all calculations.[16] The total energy was obtained by solving the Kohn−Sham equations of the local density approximation with the Perdew−Zunger exchange-correlation functional.[17] The results were corrected for nonlocality within the generalized gradient approximation with the Perdew−Wang 91 functional.[18] VASP uses the plane-waves basis set and pseudopotentials.[19] A cutoff energy of 300 eV was used. Brillouin zone sampling was restricted to the Γ point. A quasi-Newton forces-minimization algorithm was employed for all calculations. Convergence was assumed to be achieved when forces were below 0.05 eV/Å.

The transition-state (TS) search method employed by VASP is the nudged elastic band (NEB) method.[20] Several images of the system are defined along the investigated reaction pathway. These images are optimized by allowing a relaxation in the subspace perpendicular to the reaction coordinate. Once all forces in the intermediate states fall below 0.08 eV/Å, the transition state was optimized separately. To define initial geometries of the transition-state images, we used the transition-state geometries obtained from cluster approach calculations (see ref 11).

The mordenite unit cell was the same as the one used in our previous studies.[7,14] However, we employed a unit cell for which the Si/Al ratio is 47 in the present study because we wanted to analyze the intermolecular isomerization reaction in the absence of an associative effect between catalytic active sites. In total, the unit cell box contained 172 atoms (13 C, 15 H, 1 Al, 47 Si, and 96 O). The geometry of the box was kept fixed after the mordenite box was separately optimized. The dimensions of the unit cell were $a = 13.648$ Å, $b = 13.648$ Å, $c = 15.105$ Å, $\alpha = 96.792°$, $\beta = 90.003°$, and $\gamma = 90.022°$. No constraints were used on the atomic positions within the unit cell. External active sites were not considered in our model.

The bulky diphenylmethane intermediates cannot easily be accommodated in the micropore of mordenite.[15] We checked the minimum and transition state of reaction in which a diphenylmethane intermediate is involved using dynamic annealing simulations. The simulations ran over 0.6 ps with a time step of 1 fs. The temperature was linearly decreased from 600 to 10 K every 10 steps. The cutoff energy was reduced to 280 eV for these simulations. In the transition state, the positions of the carbon atoms that were involved in the chemical bond breaking and formation were kept fixed. As previously described, the resulting system forces were minimized afterward.

3. Results

We considered as a starting situation a system in which toluene is physisorbed to the acidic proton and benzene is adsorbed nearby (see Figure 1 and **Ads** in Figure 2). The adsorption mode of toluene with respect to the acidic proton is η^2(CC). The proton−aromatic carbon atom distances were 2.54 and 2.67 Å for H_aC_6 and H_aC_7, respectively (see Table 1). Benzene adopted an η^6 adsorption mode with respect to the 12-membered ring of mordenite (see **Ads** in Figure 2). Other conformations of benzene have been computationally tested, and the η^6 adsorption mode was found to be the more stable in agreement with the findings of Demuth et al.[21] The benzene molecule did not interact with the acidic proton.

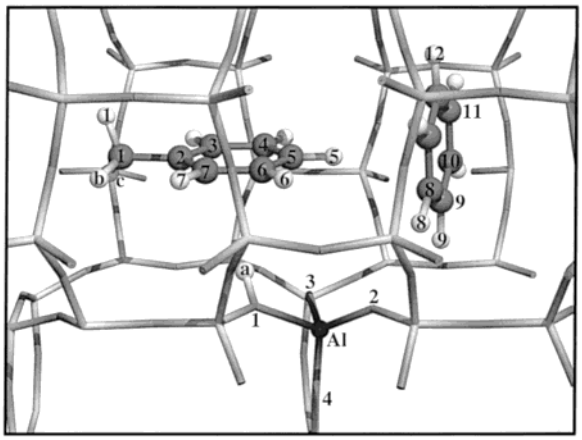

Figure 1. Geometry of toluene adsorbed to the acidic site of H-MOR and benzene in a nearby position as obtained from the periodic calculations. The labels that are used in this figure will be the same for all others geometries; these constitute the reference.

Two alternative reaction pathways are possible for this system. Both of them lead to transalkylation between toluene and benzene. In the first one, proton attack occurs on a hydrogen atom of the methyl group of toluene leading to the formation of a benzyloxy species. This reaction route is known as the disproportionation route.[9,10] In the second reaction pathway, proton attack occurs on the toluene carbon atom in the α position with respect to the methyl group.[11] This induces the methyl group to move toward benzene. This reaction pathway is a direct transalkylation route. We will consider it in more detail later.

As mentioned previously, the disproportionation reaction pathway's first transition state corresponds to a proton attack on a hydrogen atom of the toluene methyl group. As can be seen in Figure 2 (see **TS1**), the chemical nature of this transition state is very close to that of a primary carbenium ion. The formation of H_2 is already almost complete ($H_aH_1 = 0.77$ Å), whereas the zeolitic Al−O bonds are chemically equivalent ($AlO_1 = 1.73$ Å, $AlO_2 = 1.74$ Å, $AlO_3 = 1.72$ Å, and $AlO_4 = 1.72$ Å) (see **TS1** in Table 1). The acidic proton is no longer connected to the zeolitic oxygen atom ($O_1H_a = 2.32$ Å). The bond between the hydrogen atom H_1 and the methyl group carbon atom is also broken ($H_1C_1 = 2.47$ Å). The carbenium ion is in very close proximity to the deprotonated Brønsted site ($H_bO_3 = 2.03$ Å). Benzene has changed its orientation with respect to the one it adopted in **Ads**. One of its aromatic carbon atoms is relatively close to the H_2 molecule in formation ($H_1C_8 = 2.71$ Å). We previously observed that the coadsorbed benzene does not lower the activation energy.[11] The activation energy of **TS1** transition state is high with $E_{act} = 221$ kJ/mol with respect to **Ads**.

Protonated species are unstable within a zeolite.[2e,2f,8a,8b] The carbenium-like system involved in the transition state chemisorbs to the deprotonated Brønsted site through the formation of an alkoxy bond, and H_2 diffuses away. A benzyloxy species is formed in this process (see **Int1** in Figure 2). This system shows a relatively high energy with respect to **Ads** ($E_{Int1} = 157$ kJ/mol). However, this is not really surprising: in zeolite, hydrogen formation is an endothermic reaction.[1c,4] The alkoxy bond distance is similar to that of other alkoxy bonds (see **Int1** in Table 1 and ref 11). This suggests that the high energy is due to the endothermic formation of H_2. We will analyze this more closely in a later point.

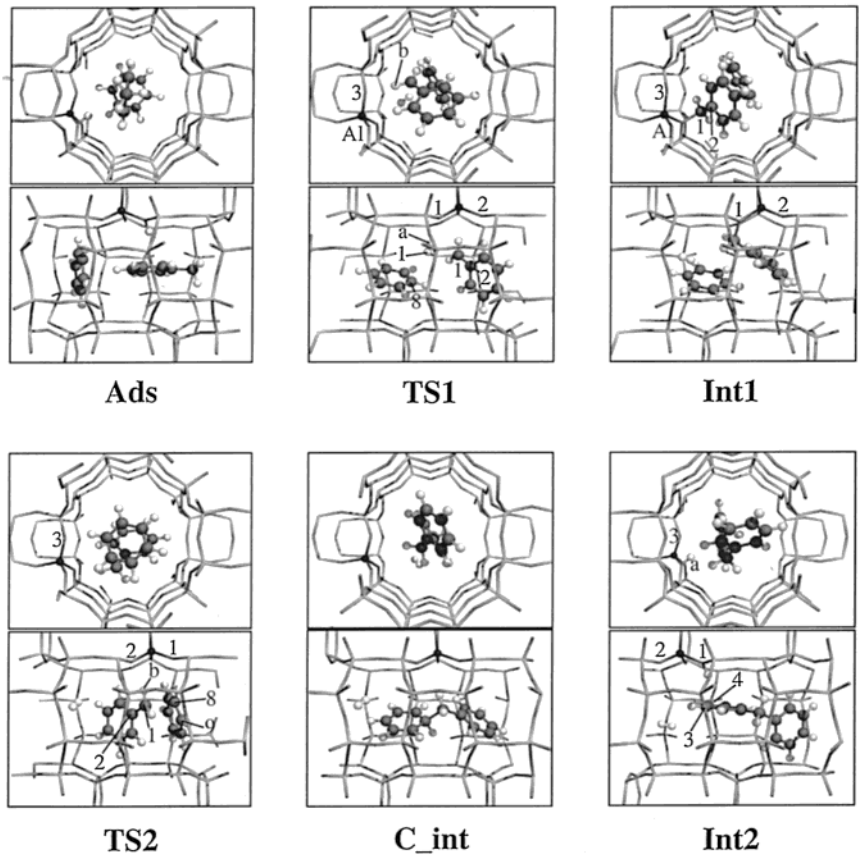

Figure 2. Front and side views of the intermediates and transition states for the disproportionation reaction pathways of toluene and benzene catalyzed by acidic mordenite as obtained from the periodic calculations.

TABLE 1: Main Geometry Parameters of the Different Systems in the Disproportionation of Toluene and Benzene Catalyzed by Acidic Mordenite as Obtained in the Periodic DFT Calculations[a]

Ads		TS1		Int1		TS2		Int2	
AlO_1	1.90	AlO_1	1.73	AlO_1	1.69	AlO_1	1.73	AlO_1	1.90
AlO_2	1.70	AlO_2	1.74	AlO_2	1.91	AlO_2	1.74	AlO_2	1.69
AlO_3	1.69	AlO_3	1.72	AlO_3	1.69	AlO_3	1.72	AlO_3	1.69
AlO_4	1.69	AlO_4	1.72	AlO_4	1.71	AlO_4	1.71	AlO_4	1.70
O_1H_a	0.99	O_1H_a	2.32	O_2C_1	1.55	O_2C_1	3.20	O_1H_a	0.99
H_aC_6	2.54	H_aH_1	0.77	H_aH_1	0.74	C_1C_8	2.20	H_aC_3	2.66
H_aC_7	2.67	H_1C_1	2.47	AlO_1C_1	116.6	O_2H_b	2.18	H_aC_4	2.49
O_2H_8	2.40	H_bO_3	2.04	$O_1C_1C_2$	113.3	O_1H_8	2.29	AlO_1H_a	109.7
$O_2H_8C_8$	150.6	H_1C_8	2.71	$AlO_1C_1C_2$	43.2	AlO_2C_1	100.1	$O_1H_aC_3$	147.4
AlO_1H_a	108.5	AlO_1H_a	106.3			$O_2C_1C_2$	101.3	$O_1H_aC_4$	153
$O_1H_aC_6$	139.2	$O_1H_aH_1$	173.4			$O_2H_bC_1$	154.0	$AlO_1H_aC_3$	−137.8
$O_1H_aC_7$	149.4	$H_aH_1C_1$	92.3			$O_1H_8C_8$	131.0	$AlH_aC_3C_4$	127.7
		$H_1C_1C_2$	112.7			$O_2H_bC_1C_2$	12.2		
						$O_1H_8C_8C_9$	11.5		
						$AlO_2C_1C_2$	−105.4		
						$AlO_1C_8C_9$	54.7		

[a] Distances in Å, angles in deg. Description of atomic labels is in Figures 1 and 2.

The unstable benzyloxy species then desorbs from the Brønsted site oxygen atom. This generates a carbenium ion, which then attacks an aromatic carbon atom of benzene (see **TS2** in Figure 2). The carbon−carbon bond formed has a bond length of $C_1C_8 = 2.20$ Å in the transition state (see **TS2** in Table 1), whereas the alkoxy bond has already been broken ($O_2C_1 = 3.20$ Å). Both the carbenium ion and benzene interact through their hydrogen atoms with oxygen atoms of the deprotonated Brønsted site ($O_2H_b = 2.18$ Å, and $O_1H_8 = 2.28$ Å). The activation energy of the diphenylmethane formation is $E_{act} = 193$ kJ/mol with respect to the **Ads** system.

After C−C bond formation, a diphenylmethane carbocation is formed (see **C_int** in Figure 2). This system is not a minimum. The energy of this system is only 3 kJ/mol below the energy of **TS2**. Reorientation of protonated diphenylmethane so as to allow proton back donation to the depronated Brønsted is hindered for such a bulky molecule within the micropore of mordenite.[9,10] This system illustrates that transition-state energies can be close to the related ionic complex energy.[1c,2e,2f]

The proton is back-donated to the Brønsted site without an activation energy barrier, and diphenylmethane is formed (see **Int2** in Figure 2). Diphenylmethane adopts an η^2 adsorption mode with respect to the acidic proton. Two carbon atoms of one of the aromatic rings of diphenylmethane interact with the acidic proton ($H_aC_3 = 2.66$ Å and $H_aC_4 = 2.49$ Å) (see **Int2** in

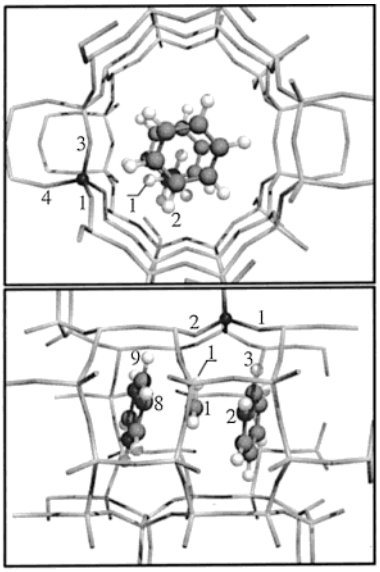

Figure 3. Front and side views of the direct transalkylation transition state between toluene and benzene catalyzed by acidic mordenite as obtained from the periodic calculations. The labels that are used in this figure are the same as those in Figure 1.

Table 1). The energy of this system is $E_{Int2} = 67$ kJ/mol with respect to the energy of **Ads**.

After **Int2** has been reached, a transition state equivalent to **TS2** is formed, which allows the transfer of the methyl group from one aromatic ring to another. One also has to mention that an alternative reaction route exists to **Int1**. An additional toluene molecule can exchange one of its methyl protons with the benzyloxy species.[1,9d] This hydride transfer reaction avoids the highly energetic transition state **TS1**. We have discussed the hydride transfer TS in another study,[11] and we will thus not expand upon it here.

Another reaction pathway is followed to achieve intermolecular isomerization of toluene by reaction with benzene. Toluene becomes protonated at an aromatic carbon atom in the α position with respect to the methyl group. The activated molecule changes its orientation so as to present its methyl group to benzene, and then methyl group jump occurs (see **TS_dt** in Figure 3). Such a mechanism, which can be qualified as direct transalkylation, is highly similar to the mechanism of methylation of toluene with methanol (see ref 7). In the present transition state, the methyl carbocation is sandwiched between the two aromatic molecules. It is located in an intermediate location between the aromatic carbon atoms to which it was connected and to which it will connect ($C_1C_2 = 2.29$ Å, $C_1C_8 = 2.26$ Å, and $C_2C_1C_8 = 171.0°$) (see Table 2). The jumping methyl group is orientated such that one of its hydrogen atoms interacts with an oxygen atom of the deprotonated Brønsted site ($H_1O_2 = 2.16$ Å). Meanwhile, hydrogen atoms of the aromatic molecules also interact with oxygen atoms of the Brønsted site, thereby adding to the overall stabilization of the transition state ($H_3O_1 = 2.12$ Å and $H_9O_2 = 2.63$ Å). The activation energy that is required to achieve this reaction is $E_{act} = 179$ kJ/mol with respect to **Ads**.

4. Discussion

The reaction energy diagram corresponding to the disproportionation reaction of toluene and benzene is summarized in Table 3. The first transition state of this reaction pathway is the more difficult to achieve, with $E_{act} = 221$ kJ/mol. This step constitutes the activation step of the disproportionation catalytic cycle. The continuation in the catalytic cycle requires an activation energy that is around 30 kJ/mol lower. These data are in agreement with the findings of Guisnet et al.[9d] They experimentally observed that the disproportionation catalysis is initiated by the most reactive catalytic sites. Continuation does not require strong acid sites.

The disproportionation reaction has been shown to be strongly hampered within mordenite when external active sites of the zeolite grains are deactivated.[9] As we already have knowledge of the energetics involved in the intramolecular isomerization of toluene catalyzed by mordenite[14] and of the energetics of the disproportionation catalyzed by a small zeolitic cluster model,[11] we are able to get deeper insight into the basis of zeolite transition-state selectivity.

We observed in previous studies,[11,14] in agreement with the findings of Boronat et al.,[12a] Zygmunt et al.,[12d] and Ramachandran et al.,[22] that the zeolite framework has a strong stabilizing

TABLE 2: Main Geometry Parameters of the Transition State in the Direct Transalkylation between Toluene and Benzene Catalyzed by Acidic Mordenite as Obtained in the Periodic DFT Calculations[a]

	TS_dt
AlO_1	1.73
AlO_2	1.75
AlO_3	1.71
AlO_4	1.72
C_1C_2	2.29
C_1C_8	2.26
C_2C_8	4.53
H_1O_2	2.16
H_3O_1	2.12
H_3O_2	3.43
H_3O_3	2.57
H_9O_2	2.63
$C_2C_1C_8$	171.0
$C_3C_2C_1C_8$	−128.1
$C_2C_1C_8C_9$	126.7

[a] Distances in Å, angles in deg. Description of atomic labels is in Figures 1 and 3.

TABLE 3: Computed Energies (kJ/mol) of Transition States and Intermediates of Toluene Isomerization and Alkylation

system	periodic model	source	cluster approach	source
Ads[a]	0	this study	0	11
TS1[a]	221	this study	297	11
Int1[a]	157	this study	106	11
TS2[a]	193	this study	253	11
C_int[a]	190	this study		
Int2[a]	67	this study	47	11
TS_dt[a]	179	this study	277	11
toluene methyl shift E_{act}	179	14	282	11
toluene demethylation E_{act} to benzene and methoxide	182	14	279	11
toluene methylation with methanol to *p*-xylene E_{act}	127 (93)[b]	7	167	7
toluene methylation with methanol to *m*-xylene E_{act}	151 (100)[b]	7	173	7
toluene methylation with methanol to *o*-xylene E_{act}	142 (92)[b]	7	164	7

[a] **Ads** is the energy reference for the energies. [b] The activation energy between parenthese uses as reference a local minimum that is reached immediately prior to when methylation occurs. In this way, one estimates the steric constraints destabilization to the transition state within the mordenite micropore (34, 51, and 50 kJ/mol for *p*-, *m*-, and *o*-xylene formation transition states, respectively). The methods that have been used to obtain the results presented in this table are described in the Methods section and in refs 7,11, and 14.

SCHEME 1: The Principle of the Polanyi−Brønsted Relation[a]

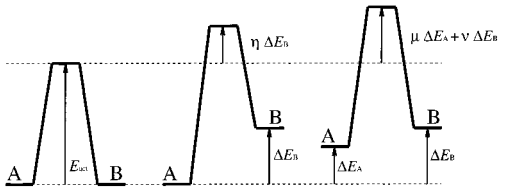

[a] Changes in reactant or product energy linearly affect the activation energy.

effect on transition states. The stabilization appears to be rather uniform when cluster approach results and periodic calculations results are compared.[11,12a,14] This stabilization was of the order of 100 kJ/mol for the intramolecular isomerization of toluene. We also report in Table 3 the data that have been obtained by means of the cluster approach method for the disproportionation reaction pathway.[11] Boronat et al.[12a] mentioned in their study that neutral system energies are unaffected by a zeolite embedding procedure. We obtained a similar result in our previous calculations. However, the situation is different here. One notes an increase of the energy level of **Int1** of around 50 kJ/mol (see Table 3). The destabilization energy is of the order of 20 kJ/mol in the case of the diphenylmethane intermediate system (**Int2**). The carbocation nature of the transition states in the present study is similar to those of the previous study. Therefore, one may expect stabilization of the transition state to also be of the order of 100 kJ/mol by embedding within the zeolite framework. This can be used to estimate the activation energies within a zeolite catalyst from the cluster approach data[11] (197 and 153 kJ/mol for **TS1** and **TS2**, respectively). However, these activation energies need to be corrected because steric constraints affect the energy ordering of the reaction pathways within mordenite. If one applies the empirical Polanyi−Brønsted relation (see Scheme 1)[23] using the energy differences observed for **Int1** and **Int2**, the corrected cluster approach activation energies are in surprisingly good agreement with the periodic calculation activation energies (216 and 186 kJ/mol for **TS1** and **TS2**, respectively).

These results mean that in the absence of steric contraints the activation energies for the disproportionation reaction are probably of the order of 200 and 150 kJ/mol for **TS1** and **TS2**, respectively. When transition states are not affected by steric constraints, the dependence of the apparent activation energy on the adsorption energy of reactant controls the dependence of a reaction on zeolite structure.[2f,7,24,25]

The activation energies that are required for intramolecular isomerization of toluene catalyzed by acidic mordenite are of the order of 180 kJ/mol (see Table 3).[14] Because the difference between the activation energies of intra- and intermolecular isomerization is around 13 kJ/mol, it is likely that intramolecular isomerization will be slightly preferred over the disproportionation reaction pathway when the reaction is catalyzed by mordenite. However, the estimated activation energies in the absence of steric constraints support the observation that the disproportionation reaction pathway is the dominant one within large-pore zeolites or in zeolites for which external active sites are not deactivated.

Experimentally, toluene−benzene isomerization is not well-documented. However, we are able to show that the disproportionation reaction pathway is not a likely pathway. Other alternative reaction pathways are more probable. Intramolecular isomerization reaction pathways have been studied in a previous study (see Table 3).[14] These reactions are easier than disproportionation. Finally, we investigated the direct transalkylation reaction pathway in the present study. We found that the direct transalkylation reaction pathway requires an activation energy that is of the same order of magnitude as that for intramolecular isomerization (see Table 3).

In the case of disproportionation and direct transalkylation between two toluene molecules, one can expect that steric constraints will destabilize the transition-state structures even more. In the case of the direct transalkylation reaction, it is possible to get an estimate of the energy of destabilization from that of the alkylation of toluene with methanol (see Table 3). The structure of the transition states is highly similar. From the Polanyi−Brønsted, one deduces that direct transalkylation activation energies increase by 30−50 kJ/mol dependent upon which xylene isomer is formed. Toluene intramolecular isomerization activation energies are below these values.[26] On the basis of these data, the formation of xylene from toluene preferentially will occur through dealkylation/alkylation cycles within mordenite.

5. Conclusions

In this theoretical study, we analyzed the bimolecular isomerization reaction pathways of toluene and benzene within acidic mordenite. Our results are in agreement with the experimental observations that report that the bimolecular reaction pathways are hampered by steric constraints within this zeolite. The empirical Polanyi−Brønsted relation appears to be very useful to analyze zeolite transition-state selectivity. One predicts that the disproportionation reaction pathway is the dominant reaction pathway in wide pore zeolites. Within mordenite, aromatics isomerization preferentially follows monomolecular reaction pathways.

Acknowledgment. Computational resources were partly granted by the Dutch National Computer Facilities (NCF). This work was performed within the European Research Group "Ab Initio Molecular Dynamics Applied to Catalysis", supported by the Centre National de la Recherche Scientifique (CNRS), the Institut Français du Pétrole (IFP), and the TotalFinaElf Raffinage Distributions company. X.R. thanks Dr. B. Anderson for the fruitful discussions and corrections of the manuscript. He thanks TotalFinaElf Raffinage Distributions for the financial support.

References and Notes

(1) (a) Venuto, P. B. *Microporous Mater*. **1994**, *2*, 297−411. (b) Tsai, T.-C.; Liu, S.-B.; Wang, I. *Appl. Catal. A* **1999**, *181*, 355−398. (c) Jacobs, P. A.; Martens, J. A. In *Introduction to Zeolite Science and Practice*; Van Bekum, H., Flaningen, E. M., Jansen, J. C., Eds.; Elsevier: Amsterdam, 1991; pp 445−496.

(2) (a) Breck, D. *Zeolite Molecular Sieves, Structure, Chemistry and Use*; Wiley: New York, 1974. (b) Barrer, R. M. *Zeolite and Clay Minerals as Sorbents and Molecular Sieves*; Academic Press: New York, 1978. (c) Jobic, H. *Spectrochim. Acta* **1992**, *48A*, 293−312. (d) Fricke, R.; Kosslick, H.; Lischke, G.; Richter, M. *Chem. Rev.* **2000**, *100*, 2303−2405. (e) Van Santen, R. A.; Kramer, G. J. *Chem. Rev.* **1995**, *3*, 637−660. (f) Van Santen, R. A.; Rozanska, X. In *Advances in Chemical Engineering*; Wei, J., Seinfeld, J. H., Denn, M. M., Stephanopoulos, G., Chakraborty, A., Ying, J., Peppas, N., Eds.; Academic Press: New York, 2001; Vol. 28, pp 399−437.

(3) Thomas, J. M.; Thomas, W. J. *Principles and Practice of Heterogeneous Catalysis*; VCH: Weinheim, Germany, 1997; pp 6−10.

(4) (a) Chen, N. Y.; Degnan, T. F., Jr.; Smith, C. M. *Molecular Transport and Reaction in Zeolites, Design and Application of Shape Selective Catalyst*; VCH Publishers: New York, 1994. (b) Ertl, G.; Knözinger, H.; Weitkamp, J. *Handbook of Heterogeneous Catalysis*; Wiley-VCH: Weinheim, Germany, 1997.

(5) (a) Csicsery, S. M. *Zeolites* **1984**, *4*, 202−213. (b) Fraenkel, D.; Levy, M. *J. Catal.* **1989**, *118*, 10−21. (c) Chen, N. Y.; Degnan, T. F., Jr.; Smith, C. M. *Molecular Transport and Reaction in Zeolites, Design and Application of Shape Selective Catalyst*; VCH Publishers: New York, 1994; pp 195−289.

(6) (a) Keil, F. J.; Krishna, R.; Coppens, M.-O. *Rev. Chem. Eng.* **2000**, *16*, 71−197. (b) Schuring, D.; Jansen, A. P. J.; Van Santen, R. A. *J. Phys. Chem. B* **2000**, *104*, 941−948. (c) Schuring, D.; Koriabkina, A. O.; De Jong, A. M.; Smit, B.; Van Santen, R. A. *J. Phys. Chem. B* **2001**, *105*, 7690−7698. (d) Smit, B.; Siepmann, J. I. *J. Phys. Chem.* **1994**, *98*, 8442−8452. (e) Smit, B. *Mol. Phys.* **1995**, *85*, 153−172. (f) Smit, B.; Maesen, T. L. M. *Nature* **1995**, *374*, 42−44. (g) Deka, R. C.; Vetrivel, R.; Miyamoto, A. *Top. Catal.* **1999**, *9*, 225−234. (h) Yang, L.; Trafford, K.; Kresnawahjuesa, O.; Sepa, J.; Gorte, R. J. *J. Phys. Chem. B* **2001**, *105*, 1935−1942.

(7) Vos, A. M.; Rozanska, X.; Schoonheydt, R. A.; Van Santen, R. A.; Hutschka, H.; Hafner, J. *J. Am. Chem. Soc.* **2001**, *123*, 2799−2809.

(8) (a) Haw, J. F.; Richardson, B. R.; Oshiro, I. S.; Lazo, N. D.; Speed, J. A. *J. Am. Chem. Soc.* **1989**, *111*, 2052−2058. (b) Haw, J. F.; Nicholas, J. B.; Xu, T.; Beck, L. W.; Ferguson, D. B. *Acc. Chem. Res.* **1996**, *29*, 259−267. (c) Rozanska, X.; Van Santen, R. A.; Hutschka, F. *J. Catal.* **2001**, *200*, 79−90.

(9) (a) Lanewala, M. A.; Bolton, A. P. *J. Org. Chem.* **1969**, *34*, 3107−3112. (b) Gnep, N. S.; Tejada, J.; Guisnet, M. *Bull. Soc. Chim. Fr.* **1982**, *1−2*, I4−I11. (c) Young, L. B.; Butter, S. A.; Kaeding, W. W. *J. Catal.* **1982**, *76*, 418−432. (d) Guisnet, M.; Gnep, N. S.; Morin, S. *Microporous Mesoporous Mater.* **2000**, *35−36*, 47−59.

(10) (a) Corma, A.; Sastre, E. *J. Catal.* **1991**, *129*, 177−185. (b) Corma, A.; Llopis, F.; Monton, J. B. *J. Catal.* **1993**, *140*, 384−394.

(11) Rozanska, X.; Saintigny, X.; Van Santen, R. A.; Hutschka, F. *J. Catal.* **2001**, *202*, 141−155.

(12) (a) Boronat, M.; Viruela, P.; Corma, A. *J. Phys. Chem. A* **1998**, *102*, 982−989. (b) Frash, M. V.; Van Santen, R. A. *Top. Catal.* **1999**, *9*, 191−205. (c) Sauer, J.; Sierka, M.; Haase, F. In *Transition State Modeling for Catalysis*; Truhlar, D. G., Morokuma, K., Eds.; ACS Symposium Series 721; American Chemical Society: Washington, DC, 1999; pp 358−367. (d) Zygmunt, S. A.; Curtiss, L. A.; Zapol, P.; Iton, L. E. *J. Phys. Chem. B* **2000**, *104*, 1944−1949.

(13) Milas, I.; Nascimento, M. A. C. *Chem. Phys. Lett.* **2001**, *338*, 67−73.

(14) Rozanska, X.; Van Santen, R. A.; Hutschka, F.; Hafner, J. *J. Am. Chem. Soc.* **2001**, *123*, 7655−7667.

(15) Halgeri, A. B.; Das, J. *Appl. Catal. A* **1999**, *181*, 347−354.

(16) (a) Kresse, G.; Hafner, J. *Phys. Rev. B* **1993**, *48*, 13115−13126. (b) Kresse, G.; Hafner, J. *Phys. Rev. B* **1994**, *49*, 14251−14269. (c) Kresse, G.; Furthmüller, J. *Comput. Mater. Sci.* **1996**, *6*, 15−50. (d) Kresse, G.; Furthmüller, J. *Phys. Rev. B* **1996**, *54*, 11169−11186.

(17) Perdew, J. P.; Zunger, A. *Phys. Rev. B* **1981**, *23*, 5048−5079.

(18) Perdew, J. P.; Burke, K.; Wang, Y. *Phys. Rev. B* **1996**, *54*, 16533−16539.

(19) Kresse, G.; Hafner, J. *J. Phys.: Condens. Matter* **1994**, *6*, 8245−8257.

(20) Mills, G.; Jónsson, H.; Schenter, G. K. *Surf. Sci.* **1995**, *324*, 305−337.

(21) Demuth, Th.; Benco, L.; Hafner, J.; Toulhoat, H.; Hutschka, F. *J. Chem. Phys.* **2001**, *114*, 3703−3712.

(22) Ramachandran, S.; Lenz, T. G.; Skiff, W. M.; Rappé, A. K. *J. Phys. Chem.* **1996**, *100*, 5898−5907.

(23) (a) Brønsted, N. *Chem. Rev.* **1928**, *5*, 231−338. (b) Evans, M. G.; Polanyi, N. P. *Trans. Faraday Soc.* **1938**, *34*, 11−29. (c) Van Santen, R. A. *J. Mol. Catal. A* **1997**, *115*, 405−419.

(24) Haag W. O. In *Zeolites and Related Microporous Materials, State of the Art 1994*; Weitkamp, H. G, Karge, H., Pfeifer, H., Hölderich, W., Eds.; Elsevier Science: Amsterdam, 1994; pp 1375−1394.

(25) Martens, J. A.; Jacobs, P. A. In *Handbook of Heterogeneous Catalysis*; Ertl, G., Knözinger, H., Weitkamp, J., Eds.; VCH: Weinheim, Germany, 1997; pp 1137−1149.

(26) The lowest activation energies of the intramolecular isomerization of xylene isomers are 164, 161, and 171 kJ/mol for *o*-, *m*-, and *p*-xylene, respectively.